

Effects of polymeric matrix on accelerated UV weathering properties of wood-plastic composites

Chia-Huang Lee, Ke-Chang Hung, Yong-Long Chen, Tung-Lin Wu, Yi-Chi Chien and Jyh-Horng Wu*

Department of Forestry, National Chung Hsing University, Taichung 402, Taiwan

* Corresponding author.

Department of Forestry, National Chung Hsing University,
#250, Kuo-Kuang Rd., Taichung 402, Taiwan
Phone: +886 4 22840345
Fax: +886 4 22851308
E-mail: eric@nchu.edu.tw

Abstract

The purpose of this work is to compare the weathering properties of different types of wood-plastic composites (WPCs) based on high-density polyethylene (HDPE), recycled high-density polyethylene (rHDPE-I and rHDPE-II), low-density polyethylene (LDPE), polypropylene (PP), recycled polypropylene (rPP), polystyrene (PS), and recycled polystyrene (rPS). The modulus of rupture (MOR) and modulus of elasticity (MOE) of all WPCs decreased with increasing exposure time of weathering. Of these, the rHDPE-II-based composite exhibited the highest MOR and MOE retention ratios after 2000 h of accelerated ultraviolet (UV) weathering, while the PS-based WPC had the lowest values. In addition, the carbonyl index difference (CID) of various WPCs increased significantly as a function of exposure time. Among them, the PS-based WPCs exhibited the most severe degradation due to photo-oxidation on the surface, while the degradation of PE-based WPCs was the mildest. These results are consistent with the change in the surface cracking and flexural properties of the composites. The PS-based WPCs also exhibited higher moisture diffusion coefficients. The mechanical behavior of WPCs after weathering is influenced by a combination of factors, such as surface oxidation, morphology changes, and moisture absorption.

Keywords: mechanical behavior; moisture diffusion coefficient; photo-oxidation; polymeric matrix; weathering; wood-plastic composite (WPC).

Introduction

Renewable and low-cost natural fibers have gained popularity as reinforcement materials in plastic composites – best known as wood-plastic composites (WPCs) – over the past decade. This approach has many advantages, such as low-density, low equipment abrasiveness, high stiffness

and strength, low maintenance requirements, and good biodegradability (Bledzki et al. 1998). WPCs belong to the most dynamic sectors of the plastic industry (Rothlin 2007). The global WPC market has experienced double-digit growth in North America and Europe (Ashori 2008; Lei and Wu 2010), and the volume of WPCs is predicted to increase from 129,000 tons in 2008 to 427,000 tons in 2014 (Lampinen 2010). Some WPCs for residential applications are being rapidly introduced to the marketplace, such as for decking, window framing, siding, and roof tiles. WPCs are still a topic of active worldwide research as demonstrated by the recent review of Kumar et al. (2011). The analysis of the plastic and wood moiety in WPCs (Lee et al. 2010; Windt et al. 2011) and the selection of the proper compatibilizer (Kumar et al. 2011) are frequently in focus. However, the main concern is on the durability of WPCs, which is generally poor. Fading, chalking, and strength weakening caused by environmental exposure are major problems for their outdoor application (Stark and Matuana 2004; Kiguchi et al. 2007).

Thermoplastics, such as high- and low-density polyethylene (HDPE and LDPE), polypropylene (PP), and polystyrene (PS) are the best-known WPC products (Nair et al. 2001; Harper and Wolcott 2004; Bengtsson et al. 2005). In our previous paper, the physicomechanical properties of these WPCs were determined (Lee et al. 2010). Only limited information is available on the weatherability and photodegradation of polyolefins (LDPE, HDPE, and PP) and their composites (Li 2000; Tidjani 2000; Seldén et al. 2004; Stark and Matuana 2004; Stark 2006; Kiguchi et al. 2007; Fabiyi et al. 2008; Park et al. 2008; Adhikary et al. 2010; Robert et al. 2011). There are no prior reports comparing the different weathering behaviors of WPCs.

Accelerated ultraviolet (UV) weathering is a powerful test for quality control and material certification (Fabiyyi and McDonald 2010; Shebani et al. 2012). Therefore, the aim of the present work is to demonstrate the effect of the polymeric matrix on the weathering properties of WPCs observed after a QUV accelerated weathering test. To the best of our knowledge, this is the first comparative study concerning the weathering characteristics of WPCs with different types of polymeric matrices.

Materials and methods

Preparation of wood particles

Trema orientalis (L.) Blume, a fast-growing wood species, was sampled from the experimental forest of the National Chung Hsing University in Nan-Tou County. Wood particles were prepared by

hammer-milling and sieving; particles between 24 and 32 mesh were investigated.

Plastics

Commercial virgin plastics: (1) HDPE [Unithene® LH901; melt flow index (MFI): 0.95 g/10 min; density: 0.95 g cm⁻³]; (2) LDPE (Paxothene® NA248; MFI: 46.00 g/10 min; density: 0.92 g cm⁻³); (3) PP (Globalene® PT100; MFI: 1.60 g/10 min; density: 0.90 g cm⁻³); (4) PS (Polyrex® PG-80; MFI: 4.00 g/10 min; density: 1.05 g cm⁻³). Source: these materials were purchased from USI Co. (Kaohsing, Taiwan), LCY Chemical Industry Co. (Kaohsing, Taiwan), and Chi-Mei Co. (Tainan, Taiwan). Recycled plastics: (5) Recycled high-density polyethylene (rHDPE-I) (MFI: 0.22 g/10 min; density: 0.95 g cm⁻³); (6) rHDPE-II (MFI: 0.35 g/10 min; density: 0.92 g cm⁻³); (7) recycled polypropylene (rPP) (MFI: 3.70 g/10 min; density: 0.91 g cm⁻³); (8) recycled polystyrene (rPS) (MFI: 8.71 g/10 min; density: 1.05 g cm⁻³). Source: these recycled materials were kindly supplied by Orbit Polymers Co., Ltd (Taichung, Taiwan). All plastic pellets were ground in an attrition mill to reduce their particle size to <20 mesh before composite processing.

Composite processing

Manufacturing WPCs: the flat-platen pressing process was applied, according to our previous papers (Hung and Wu 2010; Lee et al. 2010). The weight ratio of oven-dried wood particles (moisture content, MC<3%) to plastic powder was 60/40 (wt%). The expected density of the WPCs was 0.85±0.05 g cm⁻³. The WPC samples had dimensions of 300 mm×200 mm with 4 mm thickness. All WPCs were produced in a two-step pressing process as follows: (1) hot pressing at 170–200°C (170°C for LDPE; 180°C for HDPE, rHDPE-I, rHDPE-II, PS, and rPS; 200°C for PP and rPP) for 4 min; and (2) finishing by cold pressing until the temperature of the WPCs decreased to 25°C (approx. 5 min).

Mechanical analysis

The flexural properties [modulus of rupture (MOR) and modulus of elasticity (MOE)] of the composites were determined according to ASTM D790-07. MOR and MOE data were obtained by the three-point static bending test with a loading speed of 1.7 mm min⁻¹ and a span of 64 mm (specimen size: 80 mm×16 mm×4 mm). The samples were conditioned at 23°C and 50% relative humidity (RH) for a week before testing. The retention ratios of MOR and MOE of the WPCs after accelerated UV weathering were determined as follows: MOR (or MOE) retention ratio (%) = MOR_t (or MOE_t)/MOR₀ (or MOE₀)×100, where the measurements with the index 0 and *t* are for the WPC data before and after accelerated UV weathering for a time *t*, respectively.

Hydrothermal behavior

The moisture absorption behavior of WPCs was studied by exposing the samples to a humid environment, according to the method of Doan et al. (2007). Dry samples with dimensions of 80 mm×80 mm×4 mm were placed in a desiccator with saturated K₂SO₄ solution at 20°C (97% RH). The weight of the specimens was measured at different time intervals until equilibrium was reached. The diffusion constant (*D*) was determined from the following equations: $D = D_A / (1 + h/l + h/w)$, where *D_A*, *h*, *l*, and *w* are the apparent diffusion constant, the plate thickness, the length, and the width, respectively. The value of *D_A* was determined as follows:

$$D_A = \pi \times [h^2 / 16 (\%M_{\text{sat}})^2] \times [(\%M_2 - \%M_1) / (\sqrt{t_2} - \sqrt{t_1})]^2$$

where *%M₁* and *%M₂* are the percent weight gain of the plate at times *t₁* and *t₂*, respectively, and *%M_{sat}* is the percent weight gain at saturation.

Accelerated UV weathering

Instrument for the accelerated UV weathering: QUV accelerated weathering tester (Q-Panel Co., OH, USA) equipped with fluorescent UVA-340 lamps (Q-Lab Co., OH, USA), in accordance with the ASTM G 53-88 standard. Conditions: 8 h UV irradiation time was followed by 4 h water condensation (8/4 cycle) at a black panel temperature of 50±3°C.

ATR-FTIR spectral measurements

Instrument: Spectrum 100 FTIR spectrometer (Perkin–Elmer, Buckinghamshire, UK) equipped with a deuterated triglycine sulfate (DTGS) detector and a MIRacle ATR accessory (Pike Technologies, Wisconsin, USA). The spectra were collected by co-adding 32 scans at a resolution of 4 cm⁻¹ in the range from 650 to 4000 cm⁻¹. Five spectra were acquired at r.t. for each sample, yielding 25 spectra for each composite. The carbonyl index (CI) was calculated: $(CI) = (I_{1732} / I_p) \times 100$, where *I_p* represents the specific peak intensity of the plastic (HDPE, LDPE, PP: 2916 cm⁻¹; PS: 696 cm⁻¹) (Stark et al. 2004; Lee et al. 2010). The carbonyl index difference (CID) was also calculated: $CID = CI_w - CI_0$, where *CI₀* and *CI_w* are the carbonyl indices of the composite before and after UV weathering, respectively.

DSC and thermal analysis

Instrument: DSC-7 (Perkin–Elmer, Buckinghamshire, UK). The samples (ca. 1 mg) were encapsulated in aluminum pans and heated from 50°C to 250°C at a heating rate of 10°C min⁻¹ under N₂ flow (20 ml min⁻¹). The crystallinity of the plastic (*X_c*) was determined according to Zou et al. (2008) and calculated as: $X_c = \Delta H_m / \phi \Delta H_m^0 \times 100$, where ΔH_m is the experimental heat of fusion determined from the DSC measurement, ΔH_m^0 is the assumed heat of fusion of the fully crystalline plastic (HDPE and LDPE: 293 J g⁻¹; PP: 148 J g⁻¹), and ϕ is the weight fraction of plastic in the composites.

Measurement of surface color

Instrument: Minolta CM-3600d (Tokyo, Japan) equipped with a D₆₅ light source with a test-window diameter of 8 mm. The *X*, *Y*, and *Z* tristimulus values of all specimens were obtained directly from the colorimeter. Based on these data, the *L** (value on the white/black axis), *a** (value on the red/green axis), *b** (value on the blue/yellow axis), and ΔE^* (the color difference, $\Delta E^* = [(\Delta L^*)^2 + (\Delta a^*)^2 + (\Delta b^*)^2]^{1/2}$) color parameters were calculated, as established by the Commission Internationale de l'Eclairage (CIE) in 1976 (Wu et al. 2005).

Scanning electron microscopy

SEM instrument: Hitachi TM-1000 (Tokyo, Japan) with an accelerating voltage of 15 kV. All specimens were viewed perpendicular to the surface.

Analysis of variance

All results are expressed as the mean±SD. The significance of difference was calculated by Scheffe's test, and P-values <0.05 were considered to be significant.

Results and discussion

Color changes

The CIE $L^*a^*b^*$ color specifications are presented in Figure 1. Figure 1a shows that the ΔE^* values of all WPCs generally increased with increasing exposure time. Among the eight types of WPCs, the WPC_{PP} exhibited the most severe color changes. The value of ΔE^* changed significantly, increasing linearly to 14.4 in the first 750 h and then leveling off. In contrast, the WPC_{rHDPE-II} has the best color stability; the value of ΔE^* was <3.5 ($\Delta E^* < 3$ indicates a color difference that is not detectable by the human eye) after accelerated UV weathering for 2000 h. The effect of weathering on ΔL^* is presented in Figure 1b. Except for the WPC_{PS} and WPC_{rPS}, weathering clearly resulted in lightening, and the trend of ΔL^* is similar to that of ΔE^* . Relative to virgin plastics, most recycled plastics exhibit less color change. Probably, the additives or impurities in recycled plastics have a significant protective effect against photo discoloration. On the other hand, as visible in Figure 1c, the Δa^* value of all composites appeared to increase with increasing exposure time, through 100 h. However, after 100 h of exposure, except for the PS and rPS composites, the Δa^* value gradually decreased as a function of time. The Δb^* value displayed the same trend for all of the blends, and the WPC_{PS} and WPC_{rPS} exhibited the most severe b^* changes. After accelerated UV weathering for 2000 h, the Δb^* values of both WPCs reached approximately 10 (Figure 1d). Accordingly, the photo-sensitive aromatic groups in the side chain of some polymers (i.e., PS and rPS) lead to surface yellowing upon UV exposure.

Surface characteristics

The surface characteristics of WPCs also changed significantly after weathering. Many authors observed cracks on the surface of WPCs during natural or accelerated weathering (Li 2000; Seldén et al. 2004; Stark and Matuana 2004; Kiguchi et al. 2007; Chaochanchaikul et al. 2012). SEM micrographs in Figure 2 of WPC_{HDPE} after accelerated UV weathering for 0, 100, 1000, and 2000 h reveal coarsening of the initially smooth surfaces. The effect was visible after 100 h, and the coarsening was followed by matrix cracks and interfacial defects upon extended weathering time to 2000 h. Similar trends were also observed for other composites (Figure 3). The HDPE-, rHDPE-I-, and rHDPE-II-based WPCs suffered less crack formation after 2000 h of exposure. In other words, the weatherability of the WPCs made with virgin or recycled HDPE is better than that of other WPCs. Furthermore, the interfacial defects between the wood particles and the polymeric matrix appeared to be more severe for both WPC_{PS} and WPC_{rPS} than for other plastics.

Flexural properties

The flexural properties of various WPCs varied as a function of weathering time. As listed in Table 1, the flexural MOR and MOE of all composites generally decreased with increasing weathering time. After 2000 h, the MOR retention ratios of the WPCs are rHDPE-II (85%)>LDPE (78%)>rHDPE-I (77%)>HDPE (70%)=PP (70%)>rPP (69%)>PS (51%)>rPS (43%). Of these, the polyethylene-based WPCs, particularly the rHDPE-II composite, retained the greatest strength over

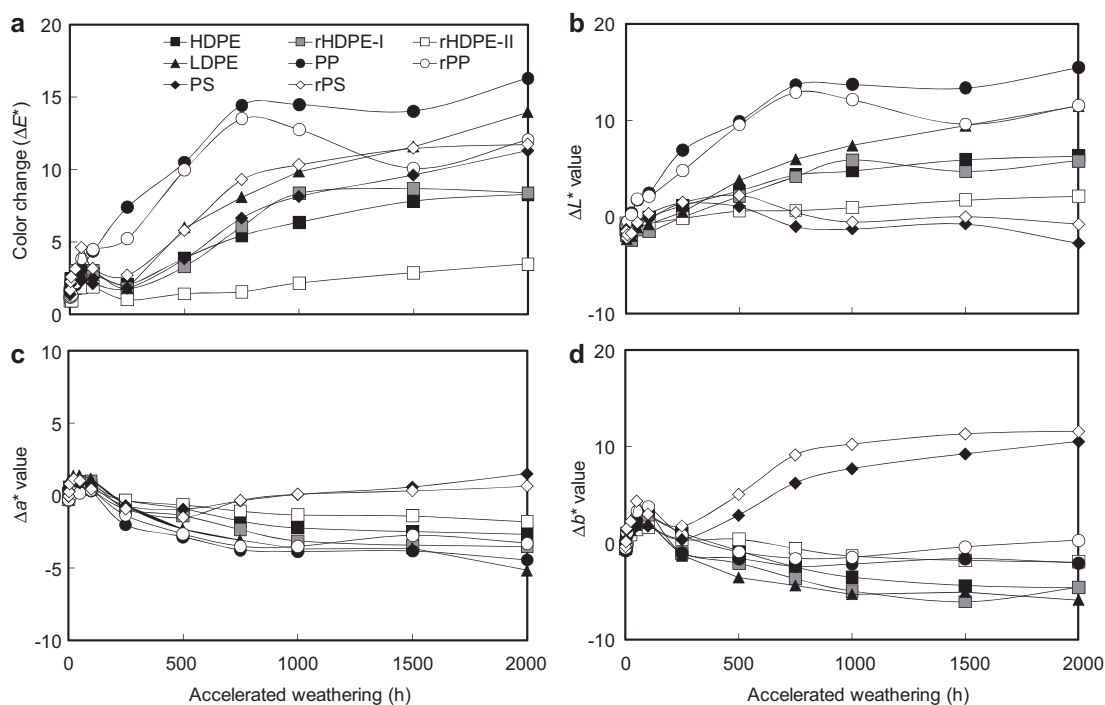


Figure 1 Changes in color parameters of various WPCs as a function of accelerated UV weathering time ($n=5$).

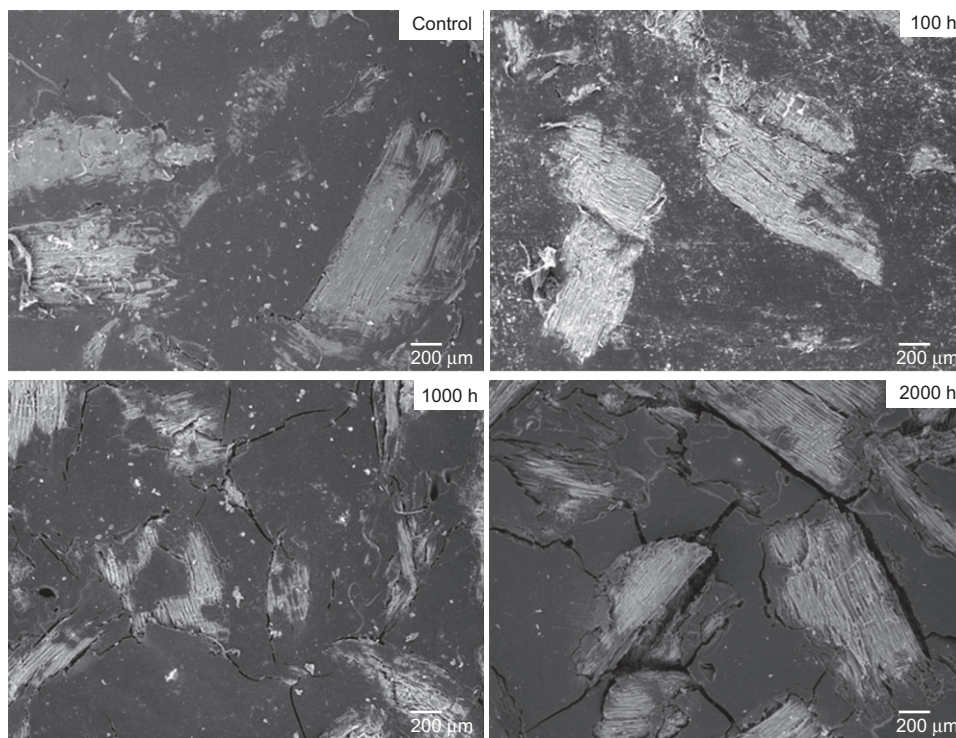


Figure 2 SEM micrographs of HDPE-based WPC after accelerated UV weathering for 0 (control), 100, 1000, and 2000 h, respectively.

the weathering period, while the polystyrene-based WPCs retained the least. Similar to the trend observed for the flexural strength, the MOE retention ratios of all WPCs were rHDPE-II (63%)>rHDPE-I (55%)>LDPE (52%)=HDPE (52%)>PP (50%)>rPP (46%)>PS (42%)>rPS (33%) after 2000 h. Corresponding to the color change results and SEM, both the PS and rPS composites showed the greatest attenuation of flexural properties during the weathering process. In general, the mechanical properties of the WPCs were not only influenced by the nature of the wood and plastic materials but also by the interfacial adhesion of the composites. Doan et al. (2007) reported that improving the interfacial adhesion between the wood fibers and the matrix led to lower values of the equilibrium water content and the diffusion coefficient. Table 1 shows that the moisture diffusion coefficients of the eight WPCs are PS>rPS>rHDPE-II>rHDPE-I=PP>rPP>HDPE>LDPE. The PS- and rPS-based composites have significantly higher moisture diffusion coefficients than the other composites. Accordingly, poor interfacial adhesion is another major reason for the reduction of flexural properties observed in WPC_{PS} and WPC_{rPS}. The majority of flexural MOR and MOE changes occurred during the first 1000 h (Table 1). These results are similar to those in the report by Stark et al. (2004), who investigated the loss in MOR and MOE for 50% wood flour-reinforced HDPE composites after weathering.

Matrix crystallinity

Cross-linking and chain scission can occur in polyolefins during weathering, which are leading to apparent differences

in the crystallinity of samples. In this study, the matrix crystallinity of various WPCs was calculated from the melting endotherms obtained from DSC. Accordingly, the “heat of fusion” of fully crystalline polymers was sought for. The polystyrene in focus is an amorphous polymer. Moreover, the crystallinity of the PS and rPS in the composites cannot be evaluated because of the lack of melting enthalpy data for 100% crystalline PS. Taking $\Delta H_m^0=293 \text{ J g}^{-1}$ and 148 J g^{-1} for PE (Khumalo et al. 2010) and PP (Beg and Pickering 2008), respectively, the matrix crystallinities of the six WPCs with known ΔH_m^0 values were determined as a function of weathering time (Table 2). The crystallinity of the various matrices significantly increased during the first 1000 h of exposure. A plateau was reached during further weathering to 2000 h, except for the rHDPE-I and rPP composites. The literature reports similar results (Kaci et al. 2001). Zou et al. (2008) claimed that the increase in crystallinity could be useful as an indicator for polymer chain scission during photo-oxidative degradation. According to this interpretation, it can be stated that the crystallinity increments observed in the present investigation are due to chain scission in the amorphous phase of the polymer. The resulting shorter molecules may have sufficient chain mobility to facilitate secondary crystallization, which leads to crack initiation (Figure 2) (Jabarin and Lofgren 1994). However, as chain scission was proceeding, the tie molecules became affected, and the crystallinity was decreased. Table 2 shows that the crystallinity of the rHDPE-I and rPP matrices decreased significantly between 1000 and 2000 h of weathering.

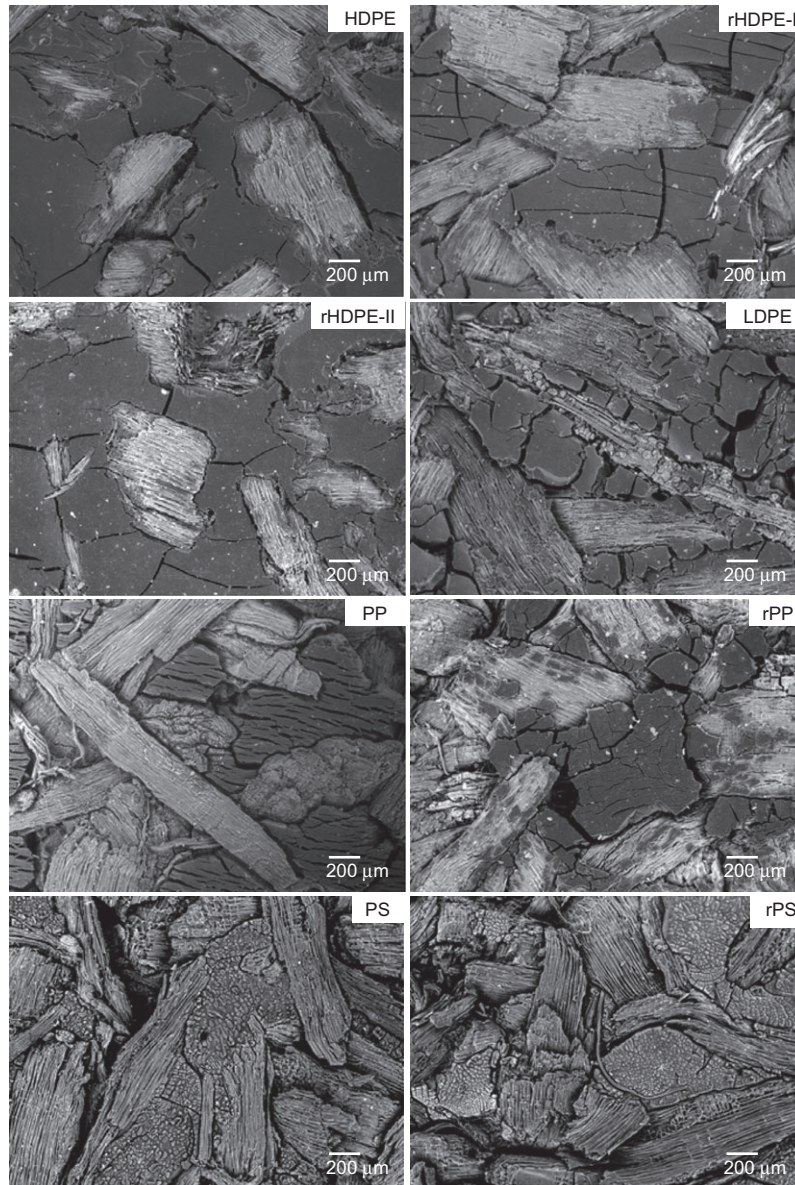


Figure 3 SEM micrographs of various WPCs after accelerated UV weathering for 2000 h.

Table 1 The moisture diffusion coefficient (D) and retention ratios in terms of MOR and MOE of various WPCs after accelerated UV weathering for different treatment times.

WPC	$D \times 10^{-6}$ ($\text{mm}^2 \text{s}^{-1}$)	MOR (MPa)	MOR retention ratio (%)				MOE (GPa)	MOE retention ratio (%)			
			100 h	500 h	1000 h	2000 h		100 h	500 h	1000 h	2000 h
HDPE	1.08 ± 0.24^B	22.5 ± 1.0^{ABC}	98 ± 1^a	84 ± 3^b	82 ± 4^b	70 ± 3^c	1.5 ± 0.1^C	89 ± 2^a	63 ± 6^b	65 ± 7^b	52 ± 4^c
rHDPE-I	1.29 ± 0.09^B	20.4 ± 1.8^{CD}	109 ± 2^a	91 ± 4^b	91 ± 3^b	77 ± 2^c	1.6 ± 0.2^C	98 ± 4^a	69 ± 7^{ab}	72 ± 11^b	55 ± 5^c
rHDPE-II	1.35 ± 0.13^B	20.8 ± 0.5^{BCD}	102 ± 5^a	94 ± 4^{ab}	88 ± 4^{bc}	85 ± 5^c	1.5 ± 0.1^C	84 ± 8^a	68 ± 3^b	70 ± 11^{ab}	63 ± 7^b
LDPE	0.56 ± 0.14^C	10.0 ± 0.3^E	90 ± 2^a	87 ± 4^{ab}	87 ± 6^{ab}	78 ± 6^b	1.0 ± 0.1^D	76 ± 7^a	53 ± 4^b	63 ± 8^b	52 ± 6^b
PP	1.29 ± 0.16^B	24.4 ± 1.5^{AB}	92 ± 3^a	84 ± 3^b	79 ± 3^b	70 ± 4^c	2.0 ± 0.1^B	82 ± 4^a	56 ± 4^b	55 ± 4^b	50 ± 5^b
rPP	1.23 ± 0.20^B	24.8 ± 1.2^A	99 ± 6^a	80 ± 5^b	73 ± 6^b	69 ± 8^b	2.3 ± 0.1^{AB}	81 ± 11^a	55 ± 4^b	47 ± 6^b	46 ± 4^b
PS	2.07 ± 0.08^A	20.9 ± 2.2^{BCD}	102 ± 3^a	63 ± 3^b	59 ± 8^b	51 ± 10^b	2.4 ± 0.1^A	80 ± 5^a	49 ± 8^b	46 ± 7^b	42 ± 9^b
rPS	1.95 ± 0.20^A	18.7 ± 1.8^D	97 ± 8^a	64 ± 4^b	48 ± 7^c	43 ± 6^c	2.2 ± 0.2^{AB}	82 ± 3^a	45 ± 3^b	39 ± 7^{bc}	33 ± 7^c

Values are the mean \pm SD ($n=5$). Different capital and lowercase superscript letters indicate significant differences ($P < 0.05$) within a column and a row, respectively.

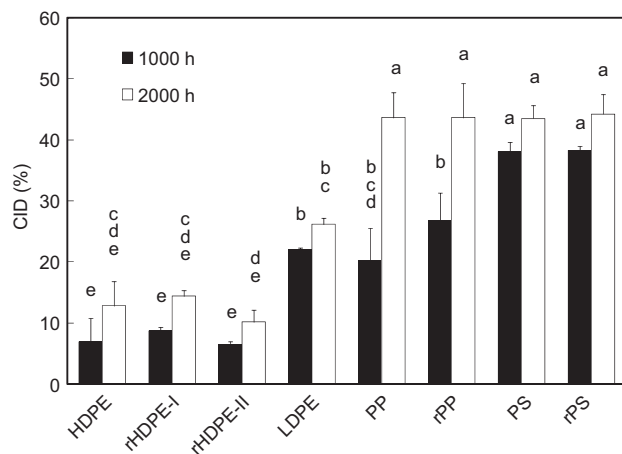
Table 2 The matrix crystallinity of various WPCs after accelerated UV weathering for different times.

WPC type	Crystallinity (%)			
	0 h	100 h	1000 h	2000 h
HDPE	20.5±1.0 ^b	20.4±0.3 ^b	57.0±4.5 ^a	56.4±0.5 ^a
rHDPE-I	22.7±0.6 ^c	22.1±0.1 ^c	60.5±1.4 ^a	49.2±6.1 ^b
rHDPE-II	26.5±1.5 ^b	25.7±4.8 ^b	31.6±1.2 ^{ab}	35.5±0.5 ^a
LDPE	11.6±0.8 ^c	9.7±2.0 ^c	14.3±0.5 ^b	19.3±1.3 ^a
PP	18.4±1.4 ^a	16.7±0.8 ^a	31.7±10.7 ^a	28.2±6.0 ^a
rPP	18.5±2.1 ^b	21.8±14.7 ^b	49.2±6.9 ^a	29.4±4.9 ^b

Values are the mean±SD ($n=3$). Different superscript letters within a row indicate significant difference at $P<0.05$.

ATR-FTIR analysis

The photostability of polyolefins is strongly dependent on the degree of oxidation during weathering (Tidjani 2000; Stark and Matuana 2004). During UV irradiation, chain scission can be induced by photodegradation via Norrish I and II reactions, as indicated by an increase in the concentration of carbonyl and vinyl groups. Figure 4 shows the carbonyl index difference (CID) of various WPCs for 1000 and 2000 h irradiation time. The CID value of all WPCs increased with increasing exposure time, and there are no significant differences between the virgin and recycled WPCs upon weathering. Others also found a similar increasing CID trend (Fabiyyi et al. 2008; Ndiaye et al. 2008). Of all WPCs in this study, the polystyrene-based WPCs exhibited the highest CID value, while the polyethylene-based WPCs had the lowest. The polystyrene composites are less photostable than the polyolefin composites. These data are also consistent with the change in the composite morphology (Figure 3) and flexural properties (Table 1). In summary, if UV weathering leads to high CID values, this is a sign for severe photodegradation (chain scission processes). An increase in crystallinity indicates the degradation of the amorphous moiety of the polymer. This process is attended by microcrack

**Figure 4** CID of various WPCs after accelerated UV weathering for 1000 and 2000 h. Values are the mean±SD ($n=5$). Bars with different letters indicate significant differences at $P<0.05$.

formation and a decrease in flexural properties due to the poor interfacial adhesion and stress transfer.

Conclusions

The physicochemical and UV weathering properties of WPCs are greatly influenced by the type of plastic utilized. Of all WPCs in this study, the rHDPE-II-based composite exhibited the highest MOR and MOE retention ratios after 2000 h of accelerated UV weathering, while the PS-based WPC had the lowest ratios. In addition, the color change of the rHDPE-II-based composite was the lowest. Accordingly, the rHDPE-II-based composite has better weathering properties than the others. The PS- and rPS-based composites have a higher moisture diffusion coefficient, which leads to greater moisture penetration and degradation of the interface between the wood and the plastic matrix. This lowers the weathering resistance. The weathering properties of the recycled composites are superior to those of virgin ones.

Acknowledgements

This work was financially supported by a research grant from the Forestry Bureau of the Council of Agriculture (100AS-5.4.2-FB-e1) and in part by the National Science Council (NSC 100-2313-B-005-019).

References

- Adhikary, K.B., Pang, S., Staiger, M.P. (2010) Effects of the accelerated freeze-thaw cycling on physical and mechanical properties of wood flour-recycled thermoplastic composites. *Polym. Compos.* 31:185–194.
- Ashori, A. (2008) Wood-plastic composites as promising green-composites for automotive industries! *Bioresour. Technol.* 99:4661–4667.
- Beg, M.D.H., Pickering, K.L. (2008) Reprocessing of wood fibre reinforced polypropylene composites. Part I: Effects on physical and mechanical properties. *Composites A* 39:1091–1100.
- Bengtsson, M., Gatenholm, P., Oksman, K. (2005) The effect of crosslinking on the properties of polyethylene/wood flour composites. *Compos. Sci. Technol.* 65:1468–1479.
- Bledzki, A.K., Reihmane, S., Gassan, J. (1998) Thermoplastics reinforced with wood fillers: a literature review. *Polym.-Plast. Technol. Eng.* 37:451–468.
- Chaochanchaikul, K., Jayaraman, K., Rosarpitak, V., Sombatsompop, N. (2012) Influence of lignin content on photodegradation in wood/HDPE composites under UV weathering. *BioResources* 7:38–55.
- Doan, T.T.L., Brodowsky, H., Mäder, E. (2007) Jute fibre/polypropylene composites II. Thermal, hydrothermal and dynamic mechanical behaviour. *Compos. Sci. Technol.* 67:2707–2714.
- Fabiyyi, J.S., McDonald, A.G. (2010) Physical morphology and quantitative characterization of chemical changes of weathered PVC/pine composites. *J. Polym. Environ.* 18:57–64.
- Fabiyyi, J.S., McDonald, A.G., Wolcott, M.P., Griffiths, P.R. (2008) Wood plastic composites weathering: visual appearance and chemical changes. *Polym. Degrad. Stabil.* 93:1405–1414.

- Harper, D., Wolcott, M. (2004) Interaction between coupling agent and lubricants in wood-polypropylene composites. *Composites A* 35:385–394.
- Hung, K.-C., Wu, J.-H. (2010) Mechanical and interfacial properties of plastic composite panels made from esterified bamboo particles. *J. Wood Sci.* 56:216–221.
- Jabarin, S.A., Lofgren, E.A. (1994) Photooxidative effects on properties and structure of high-density polyethylene. *J. Appl. Polym. Sci.* 53:411–423.
- Kaci, M., Sadoun, T., Cimmino, S. (2001) Crystallinity measurements of unstabilized and HALS-stabilized LDPE films exposed to natural weathering by FT-IR, DSC and WAXS analyses. *Int. J. Polym. Anal. Charact.* 6:455–464.
- Khumalo, V.M., Karger-Kocsis, J., Thomann, R. (2010) Polyethylene/synthetic boehmite alumina nanocomposites: structure, thermal and rheological properties. *Express Polym. Lett.* 4:264–274.
- Kiguchi, M., Kataoka, Y., Matsunaga, H., Yamamoto, K., Evans, P.D. (2007) Surface deterioration of wood-flour polypropylene composites by weathering trials. *J. Wood Sci.* 53:234–238.
- Kumar, V., Tyagi, L., Sinha, S. (2011) Wood flour-reinforced plastic composites: a review. *Rev. Chem. Eng.* 27:253–264.
- Lampinen, J. (2010) Trends in bioplastics and biocomposites. In: *Developments in Advanced Biocomposites*. Eds. Harlin, A., Vikman, M. VTT Technical Research Centre of Finland, Finland. pp. 12–20.
- Lee, C.-H., Wu, T.-L., Chen, Y.-L., Wu, J.-H. (2010) Characteristics and discrimination of five types of wood-plastic composites by FTIR spectroscopy combined with principal component analysis. *Holzforschung* 64:699–704.
- Lei, Y., Wu, Q. (2010) Wood plastic composites based on microfibrillar blends of high density polyethylene/poly(ethylene terephthalate). *Bioresour. Technol.* 101:3665–3671.
- Li, R. (2000) Environmental degradation of wood-HDPE composite. *Polym. Degrad. Stabil.* 70:135–145.
- Nair, K.C.M., Thomas, S., Groeninckx, G. (2001) Thermal and dynamic mechanical analysis of polystyrene composites reinforced with short sisal fibres. *Compos. Sci. Technol.* 61:2519–2529.
- Ndiaye, D., Fanton, E., Morlat-Therias, S., Vidal, L., Tidjani, A., Gardette, J.L. (2008) Durability of wood polymer composites: Part 1. Influence of wood on the photochemical properties. *Compos. Sci. Technol.* 68:2779–2784.
- Park, J.-M., Kim, P.-G., Jang, J.-H., Wang, Z., Hwang, B.-S., DeVries, K.C. (2008) Interfacial evaluation and durability of modified jute fibers/polypropylene (PP) composites using micromechanical test and acoustic emission. *Composites B* 39:1042–1061.
- Robert, M., Cousin, P., Fam, A., Benmokrane, B. (2011) Effect of the addition of modified mica on mechanical and durability properties of FRP composite materials for civil engineering. *Polym. Compos.* 32:1202–1209.
- Rothlin, O. (2007) Processing wood-plastic composites places new demands on feeders. *Plast. Addit. Compos.* 9:36–39.
- Seldén, R., Nyström, B., Långström, R. (2004) UV aging of poly(propylene)/wood-fiber composites. *Polym. Compos.* 25:543–533.
- Shebani, A., van Reenen, A., Meincken, M. (2012) Using extractive-free wood as a reinforcement in wood-LLDPE composites. *J. Reinf. Plast. Compos.* 31:225–232.
- Stark, N.M. (2006) Effect of weathering cycle and manufacturing method on performance of wood flour and high-density polyethylene composites. *J. Appl. Polym. Sci.* 100:3131–3140.
- Stark, N.M., Matuana, L.M. (2004) Surface chemistry and mechanical property changes of wood-flour/high-density-polyethylene composites after accelerated weathering. *J. Appl. Polym. Sci.* 94:2263–2273.
- Stark, N.M., Matuana, L.M., Clemons, C.M. (2004) Effect of processing method on surface and weathering characteristics of wood-flour/HDPE composites. *J. Appl. Polym. Sci.* 93:1021–1030.
- Tidjani, A. (2000) Comparison of formation of oxidation products during photo-oxidation of linear low-density polyethylene under different natural and accelerated weathering conditions. *Polym. Degrad. Stabil.* 68:465–469.
- Windt, M., Meier, D., Lehnen, R. (2011) Quantification of polypropylene (PP) in wood plastic composites (WPCs) by analytical pyrolysis (Py) and differential scanning calorimetry (DSC). *Holzforschung* 65:199–207.
- Wu, J.-H., Chung, M.-J., Chang, S.-T. (2005) Green color protection of bamboo culms using one-step alkali pretreatment-free process. *J. Wood Sci.* 51:622–627.
- Zou, P., Xiong, H., Tang, S. (2008) Natural weathering of rape straw flour (RSF)/HDPE and nano-SiO₂/RSF/HDPE composites. *Carbohydr. Polym.* 73:378–383.

Received October 4, 2011. Accepted May 8, 2012. Previously published online June 1, 2012.